Rare Metal Materials and Engineering
Volume 45, Issue 8, August 2016
Online English edition of the Chinese language journal

Available online at www.sciencedirect.com
ScienceDirect

Cite this article as: Rare Metal Materials and Engineering, 2016, 45(8): 1931-1937.

ARTICLE

Effect of Tungsten Addition on the Anti-fouling Property of the Electroless Ni-W-P Deposits

Cheng Yanhai, Cao Shuai, Hou Qingqiang, Han Dongtai, Han Zhengtong

China University of Mining and Technology, Xuzhou 221116, China

Abstract: Ternary Ni-W-P deposits were prepared on the mild steel (1015) substrate using electroless plating by varying sodium tungstate concentration. Surface morphology, microstructure, and the microhardness of electroless Ni-W-P deposits were investigated by scanning electron microscopy (SEM), X-ray diffraction (XRD) and a MH-6 Vickers diamond indenter, respectively. The results demonstrate that the bath concentration plays a significant role in obtaining ternary Ni-W-P deposits containing various composition of phosphorus and tungsten, which decides the surface morphology and the structure. Although nodular formation is a common feature of electroless Ni-W-P deposits, the increase of tungsten content decreases the phosphorus content of these deposits and hence changes the composition of the nanocrystalline phase. The co-deposition of tungsten in the deposits increases the microhardness due to the solid solution strengthening of nickel induced by tungsten in the deposits which resists regional plastic deformation. Moreover, the results of differential scanning calorimetry (DSC) show that Ni-W-P deposits with high tungsten content exhibit higher crystallization temperature. Further fouling experiments indicate that the Ni-W-P deposit surfaces with different tungsten contents inhibit the adhesion of fouling compared with the mild steel surface. The experiments also indicate that the fouling adhesion rate is intimately related to the tungsten content. However, the relationship between the fouling adhesion rate and surface roughness of the ternary Ni-W-P deposits is not found in these experiments.

Key words: Ni-W-P; microstructure; DSC; surface free energy; fouling

Fouling is usually referred to the accumulation of unwanted particles, precipitates or scales on heat transfer surfaces. It results in operational problems caused by heat transfer loss, pressure loss increase, and flow maldistribution[1-3]. Different approaches, such as fouling inhibitor and electrical energy, were used to reduce economic losses and downtimes of fouled heat exchangers [4-6]. With the introduction of environmental restrictions on biocides, the emphasis of the technological development is on deposit which can prevent or reduce the adhering of fouling through the physicochemical properties of the deposits rather than the release of biocides[7].

It has been reported that electroless Ni-P is the surface treatment procedure that is effective in reducing the foulings[8]. However, the further rigorous demands, such as high temperature and rapid flow conditions, make the application of Ni-P alloys face a big challenge because of the disadvantage of thermal stability and low micorhardness. The alloying is considered as the most effective method to improve the chemical and physical properties of binary Ni-P alloy deposits. The ternary Ni-W-P deposit has been paid considerable attention to since Pearlstein and Weightman[9] reported it firstly in 1963 because tungsten, which exhibits a relatively high microhardness and a high melting point of 3410 ^{o}C, could restrict the Ni_3P formation and the nickel crystallization. As a result, the mechanical and thermal properties of the Ni-P deposits were promoted[10]. Many investigations on electroless ternary Ni-W-P deposits were reported[11-17]. Hu et al.[18] investigated the structure and phase transformation behavior of as-deposited and

Received date: August 25, 2015
Foundation item: Fundamental Research Funds for the Central Universities (2015XKMS027); Priority Academic Program Development of Jiangsu Higher Education Institutions
Corresponding author: Cheng Yanhai, Ph. D., Associate Professor, Supervisor of Ph. D. Candidate, School of Mechanical and Electrical Engineering, China University of Mining and Technology, Xuzhou 221116, P. R. China, Fax: 0086-516-83590708, E-mail: chyh1007@163.com

heated Ni-W-P deposits on aluminium alloy. They found that even a small amount of tungsten (1.75 wt%) could significantly enhance the thermal stability of nanocrystalline structure and cause nickel lattice expansion to some extent. Balaraju et al.[19] prepared ternary Ni-W-P deposits using hypophosphite by different process parameters and found the deposits could obtain better thermal stability compared to others when the sodium tungstate concentration was 20 g/L. Wu et al.[20] studied the detailed microstructure evolution and the strengthening mechanism for ternary Ni-W-P deposits. They confirmed that the Ni-W-P deposits were hardened not only by the precipitation of Ni_3P but also by the nickel (tungsten) solid solution matrix after being heat treated. Obviously, these reports mainly focused on the effects of co-deposition of tungsten on the deposition rate, composition and deposit properties such as hardness and thermal stability. Few reports were mentioned on the effect of incorporation of tungsten in Ni-P matrix on the surface free energy and anti-fouling of ternary Ni-W-P deposits in literatures.

The present paper shows the effect of deposit composition on the anti-fouling properties as well as the mechanical properties of the deposits, such as the phase microstructure and microhardness, thermal stability. Besides, the relation between surface free energy and anti-fouling of the ternary Ni-W-P deposits were mainly investigated.

1 Experiment

The ternary Ni-W-P deposits were prepared using an electroless plating technique on mild steel samples with dimensions of 15 mm×10 mm×4 mm. The preparation process before electroless plating was mentioned in Ref.[10]. Various ternary Ni-W-P deposits were prepared using the following ingredients: nickel sulfate (18 g/L) and sodium tungstate were nickel and tungsten sources, respectively. Sodium hypophosphite (20 g/L) was the reducing agent. Sodium citrate (35 g/L) and lactic acid (15 g/L) were the complexing and ammonium acetate (12 g/L) was the buffering agent. Sodium tungstate concentration from sample 1 to sample 5 was 30, 35, 40, 45, and 50 g/L, respectively. Electroless Ni-W-P baths were operated at pH 7.8~8.2, adjusted by sodium hydroxide, and the temperature was maintained at 90±2 °C.

Surface morphology and composition of the Ni-W-P deposits were characterized by a scanning electron microscopy (SEM, Model QuantaTM250, FEI, USA) with energy spectrum analysis function. The microstructures of the deposits were characterized by X-ray diffraction (XRD, Model D8 Advance, BRUKER, Germany) with monochromatic copper Kα (λ=0.154 nm) radiation [21,22]. Microhardness was measured using a MH-6 Vickers diamond indenter on a cross-section with a load of 50 g and keeping time of 5 s. The heat loss and heat evolving during crystalline processes of the deposits were tested with a differential scanning calorimeter. The heating temperature ranged from room temperature to 700 °C under the constant heating rates of 20 °C/min for 1 h. Contact angle and surface free energy were measured by the DSA-100 instrument designed and made by Germany's KRÜSS company. Distilled water was used as the testing medium. All measurements were carried out at 26±1 °C and 45±5 % RH.

The fouling adhesion experiments were carried out in a test rig with a constant flow boiling pool at the atmospheric pressure. Tap water (without softening) was kept flowing through the container system. The fouling mass on the sample surface was measured in an electronic analytical balance with the accuracy of 10^{-4} g every 4 h. For comparison, un-coated stainless steel with the same size commonly used for heat exchanger surface was also tested under the same conditions. After the process of fouling adhesion, the surface morphology of fouling of each sample was observed by a 3D super-depth digital microscope (KEYENCE, VHX-500FE, Japan).

2 Results and Discussion

2.1 Surface morphology and X-ray diffraction results

Fig.1 presents the surface morphologies of Ni-W-P deposits prepared under different process conditions. The surface morphology of Ni-W-P deposits is rather compact without visible defects such as porosity, and shows the typical spherical nodular structure. However, sample 1 (30 g/L sodium tungstate in the bath) has a coarse deposit surface and the nodules exhibit an obvious columnar growth. When the concentration of sodium tungstate is 35 and 40 g/L, the surface morphology of deposits become smoother and a few visible nodules distribute uniformly in the surface. At higher concentrations of sodium tungstate (45 g/L), the larger nodules are observed. However, with addition of 50 g/L sodium tungstate in the bath, the size of nodular structure becomes fine.

Fig.2 shows the element compositions of the Ni-W-P deposits measured by EDS analysis. From Fig.2, it is obvious that the composition of tungsten in the as-deposited Ni-W-P increases from 3.75 wt% to 10.5 wt% whereas phosphorus content decreases from 10.3 wt% to 4.85 wt% with the increase of sodium tungstate concentration from 30 g/L to 45 g/L in the bath. However, when further increasing the sodium tungstate concentration, tungsten content decreases. These results are also in agreement with the result of Balaraju et al.[19] which indicates the increase of ratios of metals ions to hypophosphite ions in the bath. According to them, the addition of tungstate ions not only promotes the deposition of tungsten but also suppresses the

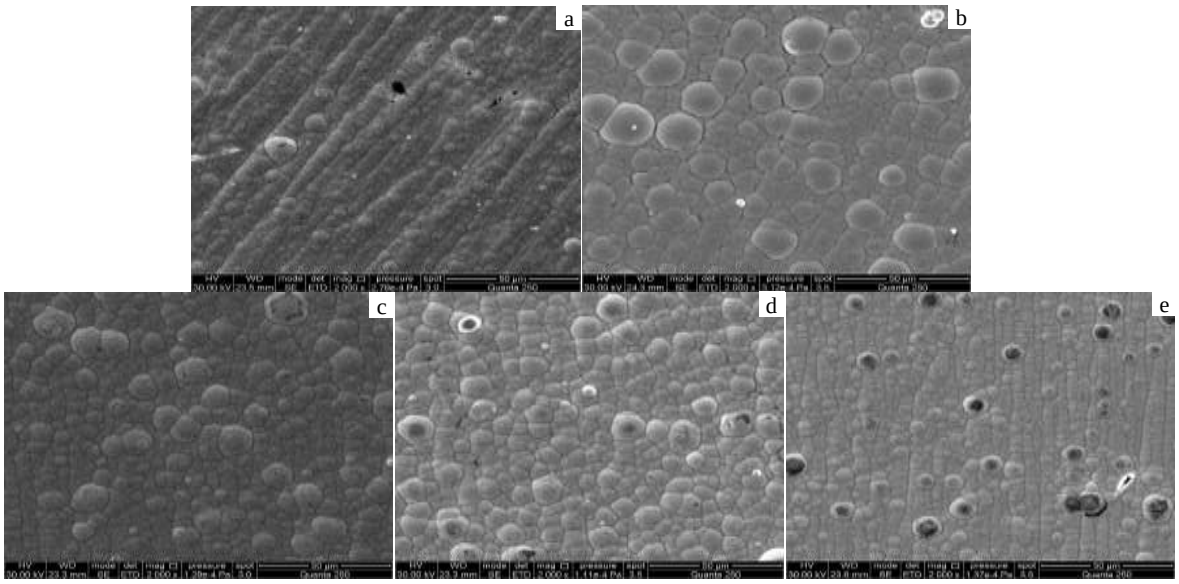

Fig.1 Surface morphologies of Ni-W-P deposit samples: (a) sample 1, (b) sample 2, (c) sample 3, (d) sample 4, and (e) sample 5

cathodic reaction of $H_2PO_2^-$, thereby decreasing the phosphorus content.

Fig.3 shows the XRD patterns of the as-plated Ni-W-P deposits obtained in different processes. The diffraction patterns indicate that all the Ni-W-P deposits are in an amorphous state. Furthermore, it can be seen that the diffraction peaks of as-deposited ternary Ni-W-P deposits become sharper and the full width at half maximum shows a narrower trend with the increase of sodium tungstate concentration in the bath. This is mainly because that the tungsten and phosphorus contents change with the variation of sodium tungstate concentration in the bath, thus affecting the microstructure of Ni-W-P deposits. Some investigators reported that crystalline state of the ternary Ni-W-P deposits mainly depends on the amount of phosphorus in the literatures[23-27]. The deposits exhibit an amorphous structure when the phosphorus content is higher than 8 wt%. However, mixture of amorphous and nanocrystalline structure could be observed when the phosphorus content is between 5 wt% and 7 wt%. When the phosphorus content is below 5 wt%, they exhibit a microcrystalline structure. So, sample 1 and 2 are almost the amorphous phase and the content of nanocrystalline phase is very low. Samples 3 may consist of mixture of amorphous and nanocrystalline phase. Besides, sample 4 and 5 exhibit a nanocrystalline structure.

2.2 Microhardness and DSC analysis

Fig.4 shows the effect of various sodium tungstate concentrations in bath on the microhardness HV of the Ni-W-P deposits. It is obvious that the microhardness increases to a maximum value of approximately 5800 MPa

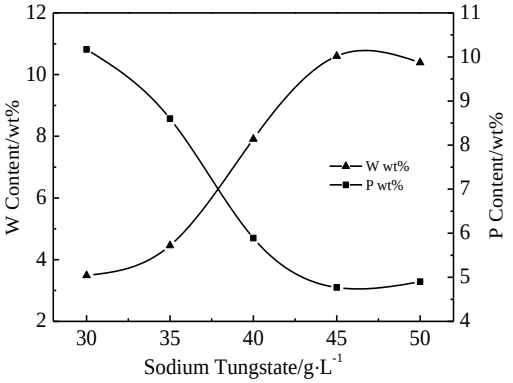

Fig.2 Effect of sodium tungstate concentration in the bath on the deposit composition

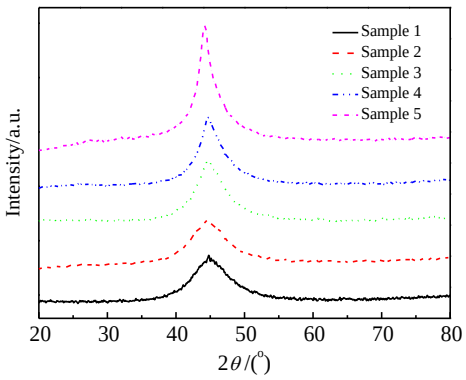

Fig.3 XRD patterns of the deposit samples

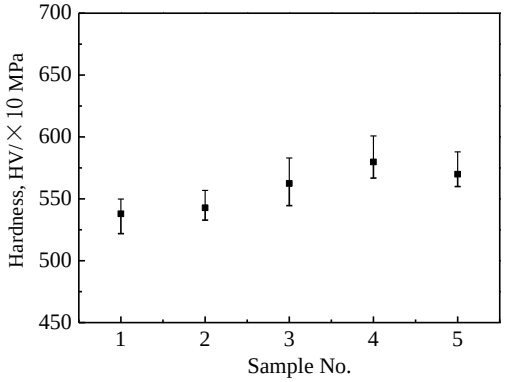

Fig.4 Microhardness of the Ni-W-P deposits samples

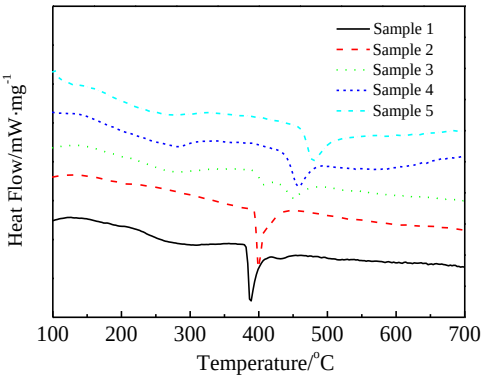

Fig.5 DSC curves of the Ni-W-P deposit samples

with the increase of sodium tungstate concentration in bath. When the concentrations of sodium tungstate increase beyond 45 g/L, the microhardness slightly decreases. This trend for microhardness seems to be in proportion with the tungsten content in the Ni-W-P deposits. It has been reported[18,19] that the Ni-W-P deposits with low phosphorus content exhibit higher microhardness in as-deposited condition due to the high internal stress. Moreover, the addition of tungsten in the Ni-W-P deposits could resist regional plastic deformation. The major contribution to the increased microhardness is the solid solution strengthening of nickel induced by tungsten in the deposits.

To find out the phase transformation behavior, DSC curves of electroless ternary Ni-W-P deposits with different contents of tungsten at a scanning rate of 20 °C/min are shown in Fig.5. The presence of exothermic peaks in the figure for all the samples is indicative of the transformation of amorphous deposits into crystalline deposits. Sample 1 exhibits a main sharp exothermic peak at 380 °C, a low temperature peak at 285 °C and a shallow peak at 430 °C whereas sample 2 shows only one main exothermic peaks at 392 °C. In the case of sample 3, there are two exothermic peaks, a low temperature peak at 278 °C, a "w" type of major exothermic peaks in range of 400~450 °C. Both sample 4 and 5 show a single but broad and shallow exothermic peak at 450 and 480 °C compared to other samples. Apart from the major exothermic peak, the very shallow and faint peaks at low temperature also appear in sample 4 and sample 5. It has been reported[10,18] that the major exothermic peak in the DSC thermograms obtained for ternary Ni-W-P deposits corresponds to the long-range atomic movements, causing precipitation of stable phases such as fcc nickel and nickel phosphide. A low temperature peak present in nanocrystalline deposits could be attributed to the structural relaxation such as annihilation of point defects and dislocations within the grains and grain boundary zones. From the above it is evident that deposit composition plays an important role on the phase transformation behavior of ternary deposits. From Fig.5, it can also be observed that the main exothermic peak shifts the higher temperature from sample 1 to 4 and has a slight down for sample 4 to sample 5. This means the crystalline temperature increased with the increase of tungsten content in the deposits.

Fig.6 shows the activation energy of all the deposits obtained by modifying Kissinger method. That higher activation energy is obtained for the low phosphorus deposits, which is due to the higher crystallization temperature[19]. From Fig.6, it is clearly seen that sample 4 has the highest tungsten content among the samples and has the highest activation energy. Therefore, incorporation of tungsten in deposits not only enhances the microhardness but also improves the thermal stability.

2.3 Contact angle and surface free energy

The wettability of the ternary Ni-W-P deposits was evaluated by contact angle measurement. Fig.7 shows the representative images of liquid droplets on the Ni-W-P deposits. Significant variations in the contact angle values were observed on the deposits. According to the contact angle values, the surface free energy of the Ni-W-P deposits was calculated using van Oss method[28].

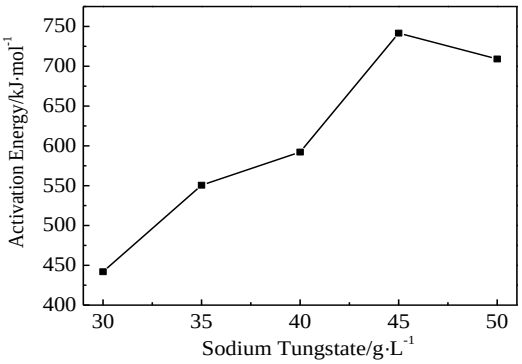

Fig.6 Effect of sodium tungstate concentration on activation energy

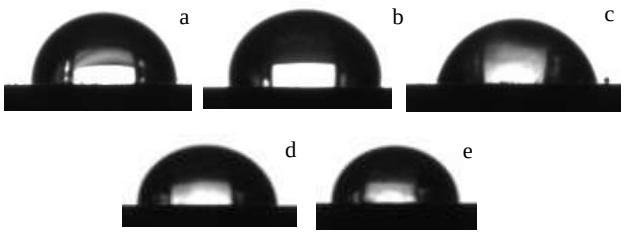

Fig.7 Representative images of liquid droplets on the Ni-W-P deposits sample 1 (a), sample 2 (b), sample 3 (c), sample 4 (d), and sample 5 (e)

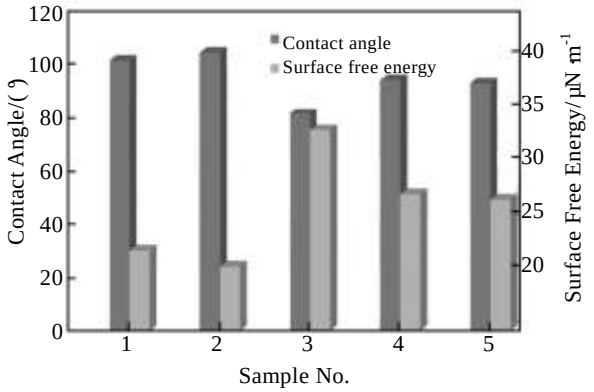

Fig.8 Contact angles and surface free energy of the Ni-W-P coating samples

Fig.8 demonstrates the contact angles and surface energy of the ternary Ni-W-P deposits. From this figure, it is evident that all of the Ni-W-P deposits whose surface free energy values are less than 35 mJ/m^2 belong to the surface with low surface free energy. But, combined with the above results about the EDS analysis, it is worth noting that the amount of the tungsten in the deposits has no marked effect on the surface free energy.

2.4 Anti-fouling property

Fig.9 shows the surface morphology of the fouling on the surfaces of ternary Ni-W-P deposits and uncoated mild steel as observed by conducting fouling adhering experiments in boiling water for 20 h. From this figure, we could see that the fouling is uniformly distributed on the ternary Ni-W-P deposit surfaces.

Fig.10 shows the relation between the fouling mass per unit area and time elapsed for the electroless Ni-W-P deposit samples and an untreated mild steel substrate sample. It is evident that the fouling adhering rate on the electroless Ni-W-P surfaces is markedly decreased in comparison with that of untreated mild steel substrate surface. We can also see that the fouling on the various ternary Ni-W-P surfaces differs from each other. More specifically, there appears to be the least fouling on the deposit surface of sample 1 and the most fouling on the deposit surface of sample 4. Combining this information with the results of surface free energy observations obtained in subsection 2.3, we speculate that the trend of fouling adhesion is not consistent with increase of the value of surface free energy. In another reference, Zhao et al. also reported[29] different results that minimal adhesion of $CaSO_4$ corresponded to a range of surface free energy. Therefore, the surface free energy is not the unique criterion for assessing the anti-fouling ability of the deposits.

In order to reveal the internal relations between the surface and anti-fouling property, we also studied the surface roughness of the ternary Ni-W-P deposit samples. Fig.11 demonstrates the surface roughness of the ternary Ni-W-P deposit samples before the fouling tests. From these

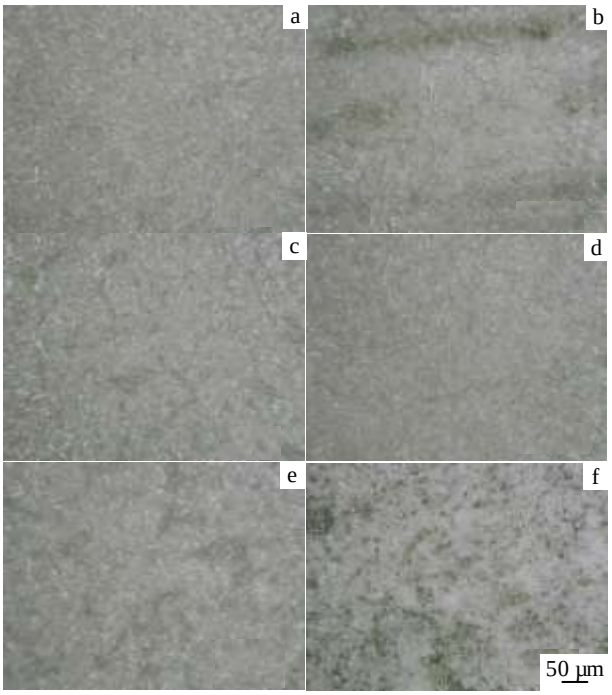

Fig.9 Fouling morphologies on the surface of different samples: (a) sample 1, (b) sample 2, (c) sample 3, (d) sample 4, (e) sample 5, and (f) mild steel

experimental results, it can be seen that there is not a necessary relationship between the fouling adhesion rate and surface roughness of the samples, but the fouling adhesion rate is intimately related to the tungsten content. Hence, it can be concluded that the tungsten content plays a significant role in the anti-fouling property of the ternary Ni-W-P deposit. The ternary Ni-W-P deposits with low tungsten content exhibit excellent anti-fouling ability. Furthermore, the anti-fouling property seems not to be improved significantly by smoothing the ternary Ni-W-P deposits. Therefore, it is of no use to polish the heat transfer surface to improve the anti-fouling property.

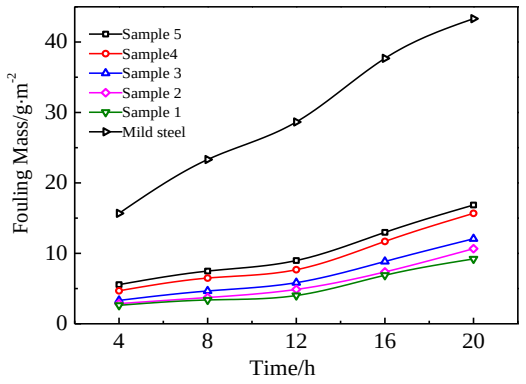

Fig.10 Fouling adhering mass versus time immersing in boiling water for different surface

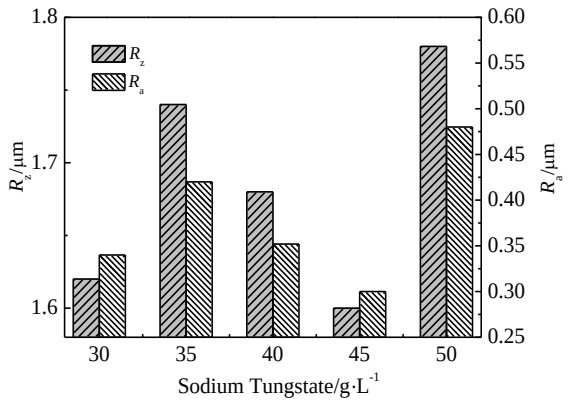

Fig.11 Surface roughness of deposit samples before fouling test

3 Conclusions

1) The bath concentration plays a significant role in obtaining various ternary Ni-W-P deposits containing phosphorus and tungsten, which in turn decides the surface morphology and the structure. Although nodular formation is a common feature of electroless Ni-W-P deposits, the co-deposition of tungsten decreases the phosphorus content of these deposits and hence changes the content of the nanocrystalline phase.

2) The addition of tungsten in the deposits can increase the microhardness due to the solid solution strengthening of nickel induced by tungsten in the deposits which resists regional plastic deformation. Moreover, deposit composition plays an important role on the phase transformation behavior of ternary deposits and the ternary Ni-W-P deposits with high tungsten content exhibit higher crystallization temperatures.

3) The Ni-W-P deposits have better anti-fouling property than the uncoated mild steel surface. The fouling adhesion rate is related to the tungsten content rather than the surface roughness. The anti-fouling property can not be significantly improved by smoothing the Ni-W-P deposits.

References

1 Krause S. *International Chemical Engineering*[J], 1993, 33: 355

2 Mayer M, Augustin W, Scholl S. *Journal of Crystal Growth*[J], 2012, 361: 152

3 Epstein N. *Heat Transfer Engineering*[J], 1983, 4: 43

4 Abd-Elhady M S, Abd-Elhady S, Rindt C C M *et al*. *Applied Thermal Engineering*[J], 2009, 29: 2335

5 Müller-Steinhagen H, Malayeri R M, Watkinson A P. *Heat Transfer Engineering*[J], 2007, 28: 173

6 Taheri A H , Sim S T V, Sim L N *et al*. *Journal of Membrane Science*[J], 2013, 448: 12

7 Miller D J, Kasemset S, Wang L *et al*. *Journal of Membrane Science*[J], 2014, 452: 171

8 Cheng Y H, Zou Y, Cheng L *et al*. *Surface and Coatings Technology*[J], 2009, 203: 1559

9 Pearlstein F, Weightman R F, Wick R. *Metal Finishing*[J], 1963, 61: 77

10 Cheng Y H, Chen H Y, Zhu Z C *et al*. *Rare Metal Materials and Engineering*[J], 2014, 43(1): 11

11 Liu H, Viejo F, Guo R X *et al*. *Surface and Coatings Technology*[J], 2010, 204: 1549

12 Liu H, Guo R X, Liu Y *et al*. *Surface and Coatings Technology*[J], 2012, 206: 3350

13 Du N, Preitzke M. *Journal of Applied Electrochemistry*[J], 2003, 33: 1001

14 Palaniappa M, Seshadri S K. *Wear*[J], 2008, 265: 735

15 Tsai Y Y, Wu F B, Chen I *et al*. *Surface and Coatings Technology*[J], 2007, 164: 502

16 Gao Y, Zhen Z J, Zhu M *et al*. *Materials Science and Engineering A*[J], 2004, 381: 98

17 Zhang W X, Huang N, He J G *et al*. *Applied Surface Science*[J], 2007, 253: 5116

18 Hu Y J, Wang T X, Meng J L *et al*. *Surface and Coatings Technology*[J], 2006, 201: 988

19 Balaraju J N, Kalavati N T, Manikandanath *et al*. *Surface and Coatings Technology*[J], 2012, 206: 2682

20 Wu F B, Tien S K, Chen W Y *et al*. *Surface and Coatings Technology*[J], 2004, 177-178: 312

21 Keong K G., Sha W, Malinov S. *Surface and Coatings Technology*[J], 2003, 168: 263

22 Chang L, Kao P W, Chen C H. *Scripta Materialia*[J], 2007, 56: 713

23 Keong K G, Sha W, Malinov S. *Materials Science and Engineering A*[J], 2004, 365: 212

24 Balaraju J N, Kalavati, Rajam K S. *Surface and Coatings Technology*[J], 2010, 205: 575

25 Keong K G., Sha W, Malinov S. *Journal of Alloys and Compounds*[J], 2002, 334: 192

26 Balaraju J N, Rajam K S. *Journal of Alloys and Compounds*[J], 2008, 459: 311

27 Cheng Y H, Chen H Y, Han D T *et al*. *Rare Metal Materials and Engineering*[J], 2014, 43(5): 1025
28 Cheng Y H, Chen H Y, Zhu Z C *et al*. *Applied Thermal Engineering*[J], 2014, 20: 43
29 Zhao Q, Liu Y, Wang C *et al*. *Chemical Engineering Science*[J], 2005, 60: 4858

钨含量对 Ni-W-P 镀层抗垢性能的影响

程延海，曹　帅，侯庆强，韩东太，韩正铜
(中国矿业大学，江苏 徐州 221116)

摘　要：采用化学镀的方法，调整化学镀工艺参数中钨酸钠的浓度，在低碳钢（1015）表面获得了钨含量不同的Ni-W-P镀层，分别采用扫描电镜、X射线衍射仪以及MH-6表面硬度计研究了钨含量对Ni-W-P镀层表面形貌、结构以及显微硬度的影响。结果表明，镀液浓度对于获得磷和钨含量起到决定性的作用，而磷和钨的含量决定了Ni-W-P镀层的表面形貌和结构。胞状晶的形成是Ni-W-P镀层的共同特征，镀层中钨含量的增加降低了磷的含量，因此改变了纳米晶相的含量。由于钨固溶于镍中诱使镀层产生固溶强化，限制了镀层局部塑性变形，从而增加了镀层的硬度。采用差热分析研究相变行为的结果表明，高钨含量的Ni-W-P镀层表现为较高的晶化温度。进一步的污垢沉积试验表明，与低碳钢表面相比，含有不同钨含量的Ni-W-P镀层表面抑制了污垢的黏附。进一步研究表明，污垢沉积速度与钨的含量有着直接的联系，而与Ni-W-P镀层表面粗糙度之间没有必然的联系。

关键词：Ni-W-P；结构；DSC；表面自由能；污垢

作者简介：程延海，男，1977 年生，博士，副教授，博士生导师，中国矿业大学机电工程学院，江苏 徐州 221116，E-mail: chyh1007@163.com